Contents

List of Figures

List of Tables

1 Theoretical background

All equations in the following chapter can be found in [1]

1.1 Law of radioactive decay

Most elements and their isotopes are stable, but neither the less some are unstable and decay over time. This phenomenon is called radioactive decay. This process is a statistical process, where the number of atoms N over time can be described with the following relation:

$$\frac{dN}{dt} = -\lambda \cdot N \tag{1}$$

Here is λ the specific decay constant for an isotope. Through integration this results in the *Law of radioactive decay*

$$N(t) = N_0 \cdot e^{-\lambda \cdot t}, \tag{2}$$

N_0 describes the number of atoms at the time 0 ($N_0 = N(0)$). The most interesting quantity of Radioactive decay is the so called Half-life $T_{1/2}$. it indicates the time, after which half of the beginning atoms have decayed.

$$N(T_{1/2}) = \frac{N_0}{2} \Longleftrightarrow T_{1/2} \overset{\tau = \frac{1}{\lambda}}{\overset{\downarrow}{=}} \tau \ln 2 \tag{3}$$

Another important quantity is the so called activity A, it is the negative change rate in the number of atoms.

$$A = -\frac{dN}{dt} = \lambda \cdot N(t) = \frac{\ln 2}{T_{1/2}} N(t) \tag{4}$$

Another quantity we will look at and also measure in this experiment is the so called rate of counts n where the number of counts is divided by the time passed:

$$n = \frac{N}{\Delta t}. \tag{5}$$

1.2 Different types of decays

There are many types of radioactive decay. The ones relevant for this experiment are $\alpha-$, β^--decay and the so called electron capture. Those will be explained shortly in the next sections.

1.2.1 α – decay

A parent nucleus X decays over time into its so called daughter nuclei Y. The common notation for nuclei and their compositions is ${}^{A}_{Z}\mathrm{X}$ where X is the element, A is the number of protons plus the number neutrons in the nucleus and Z Gives the number of protons without the neutrons. An α particle consists of two protons and two neutrons and therefore a twice positively charged He nucleus (${}^{4}_{2}\mathrm{He}$). This kind of decay mainly occurs in heavy nuclei.

The example in this experiment is the $\alpha-$decay of ${}^{147}_{62}\mathrm{Sm}$ which decays by emitting α-particles: ${}^{147}_{62}\mathrm{Sm} \rightarrow {}^{143}_{60}\mathrm{Nd} + {}^{4}_{2}\mathrm{He}$. if the count rate is known, the Half-life can be

calculated with the method explained in the following paragraphs. Considering the surface area F of a radioactive sample, one expects the rate of counts as the following:

$$n = A_V \frac{F}{4} R_{Sm_2O_3}, \tag{6}$$

$R_{Sm_2O_3}$ is the range of the active sample and $A_V = \frac{A}{V}$ the activity per volume. If we now assume that $V \underset{\text{d = thickness}}{\overset{\uparrow}{=}} F \cdot d$ and substitute Equation 4 we obtain after solving for $T_{1/2}$:

$$T_{1/2} = \frac{\ln 2 \cdot N \cdot R_{Sm_2O_3}}{4 \cdot n \cdot d} \tag{7}$$

$$T_{1/2} = \frac{\ln(2) \cdot N_{\mathrm{A}} \cdot h_{\mathrm{rel}} \cdot F \cdot R_{\mathrm{air}} \cdot \rho_{\mathrm{air}}}{2 \cdot n \cdot M_{\mathrm{Sm_2O_3}}} \cdot \sqrt{\frac{m_{\mathrm{A,Sm_2O_3}}}{m_{\mathrm{A,air}}}} \tag{8}$$

The calculations between Equation 7 and 8 can be found in the appendix subsection 5.1

1.2.2 β^- – decay

The β–emitter of this experiment is $^{40}_{19}$K. β consists of electrons and anti electron neutrinos.

$$^{40}_{19}\mathrm{K} \longrightarrow {}^{40}_{20}\mathrm{Ca} + e^- + \bar{\nu}_e$$

The Weak interaction changes with a W^-boson one down-quark into one up-quark, and therefore the neutron into a proton.

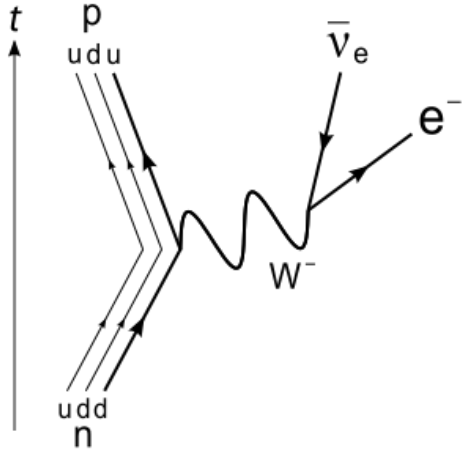

Figure 1: Feynman diagram of the β^-–decay. This picture was taken from [2]

1.2.3 Electron capture

The phenomenon of the electron capture is another way of a β^- –decay. Instead of a neutron which becomes a proton, the opposite is the case. An electron from the lower k-shell is being absorbed in the nucleus and an electron neutrino emitted. A Feynman diagram can be seen in Figure 2

$$^{40}_{19}\mathrm{K}+\mathrm{e}^- \longrightarrow {}^{40}_{18}\mathrm{Ar}+\nu_e$$

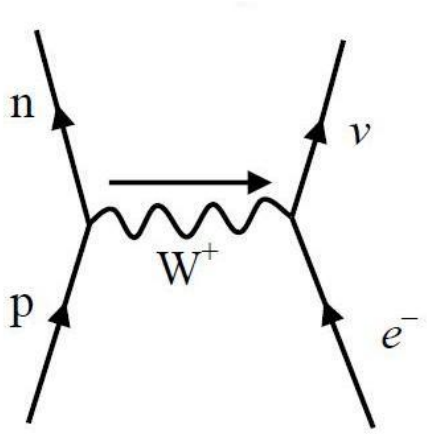

Figure 2: Feynman diagram of electron capture. This picture was taken from [3]

The process of electron capture in potassium is only 12% as likely as the β^-–decay. Therefore the decay constants need to be added up: $\lambda = \lambda_{\beta^-} + \lambda_{ec}$. Because the proportionality counter we use, can not detect electron capture so we need to make additions to our formulas:

$$\lambda = 1.12 \cdot \lambda_{\beta^-} \qquad A = N \cdot \lambda_{\beta^-} \qquad T_{1/2} = \frac{\ln 2}{1.12 \cdot A}. \tag{9}$$

With $N = \frac{m \cdot N_A}{M_{KCL}} \cdot h_{rel}$ and $A_S = \frac{A}{m}$ the specific activity we obtain for the half life the followig:

$$T_{1/2} = \frac{\ln(2)_A \cdot h_{rel}}{1.12 \cdot A_S \cdot M_{KCL}} \tag{10}$$

The specific activity A_S can be fitted with the measured data of the count rate with the following fit formula:

$$n(m) = \alpha(1 - s^{-\beta \cdot m}) \tag{11}$$

a detailed derivation of those formulas can be found in the appendix subsection 5.1

2 Setup and execution

2.1 Experimental setup

The radioactive samples, which are located in aluminium trays, are placed on a turntable in the methane flow counter. The recorded pulses are processed in various amplifiers and finally counted by the computer. The single channel analyser is used to remove noise from the actual signal.

2.2 Methane flow-counter

The counter is in a cylindrical shape and covered with lead inside, to minimise the background noise. A Molybdenum-wire is used as anode, to attract the particles. Methane is used as counter gas, it has nice counting properties and is cheap. It flows permanently through the counter to ensure that the gas keeps its counting properties. The methane flow counter works in the proportionality region (explained in subsection 2.4).

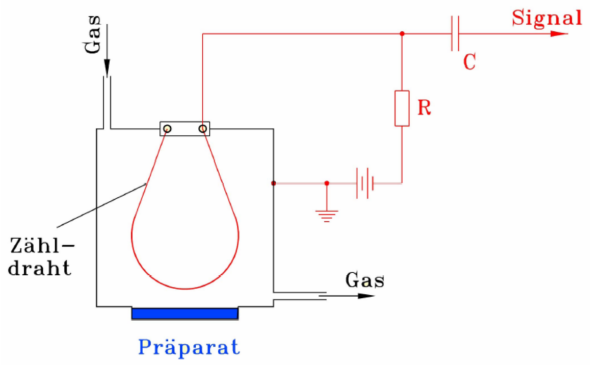

Figure 3: A schematic view of the inside of the counter, taken from [1]

2.3 Execution

At first we measured the counting characteristics of the counter with a ^{238}U in the range of 1000 V to 4000 V with steps of 100 V every 50 s and afterwards the background count rate n_b in steps of 100 V every 100 s from 1700 V to 4000 V we changed the range here, because there were no measurable counts of background beneath 2300 V.

Secondly we measured the diameter of the aluminium tray with a caliper seven times at different positions and filled it up with ^{147}Sm. We tried to make it a smooth and even surface. Afterwards the characteristics of the counter for Sm near the $\alpha-$plateau was measured between 1700 V and 3400 V. The steps where chosen as 100 V and 200 s per step. Then we estimated a good Voltage of the $\alpha-$plateau as 2300 V and measured the ^{147}Sm sample for 6000 s.

For KCL we made a similar measurement with a mass of (0.6123 ± 0.0005) g between 2800 V and 4000 V and set our working voltage to 3500 V because the count rate was significantly higher we measured only for 800 s for everyone of ten different weights. Which we measured by a precision scale with 4 digits after the comma.

2.4 Detection regions of the counter

Counters have different properties in different regions. In general a counter detects emitted radioactivity with ions, which are being released in the counting gas (in this case methane). The ionised particles are then being attracted by an anode which then sends an electric signal to the computer. A schematic setup of the used counter can be seen in Figure 3. The detection regions are mainly dependent on the voltage applied and can be split in six parts. The following picture gives an overview of those regions:

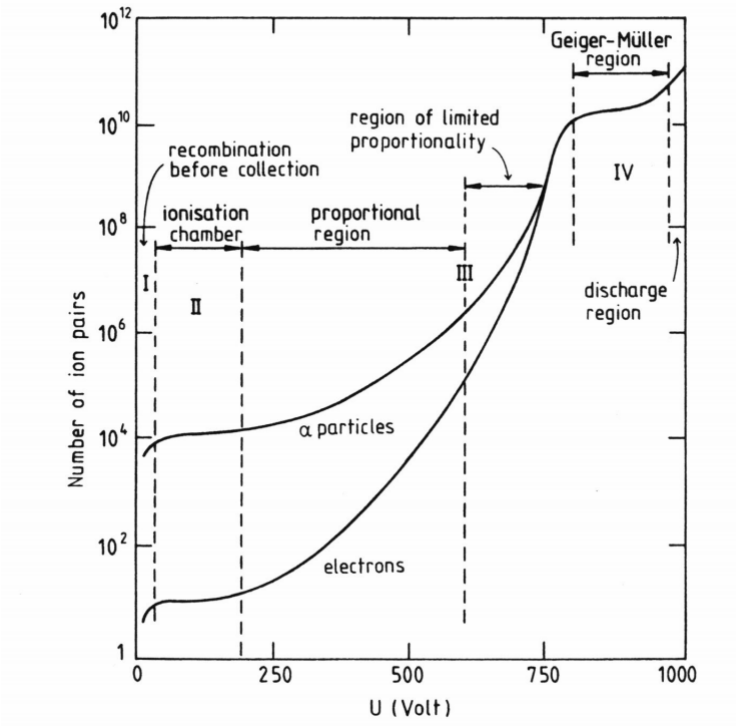

Figure 4: Characteristic of a counter Picture taken from [4]

I Is the *recombination region*. In this region the ions in the gas recombine before they reach the counter wire due to the low voltage.

II This region is called *ionisation chamber* in which the number of ions reach the saturation limit.

III The *proportional region*, in which our counter is working in. It comes to a higher rate of counts, due to secondarily produced ions. The amplitude of the signal is proportional to the primarily ionised ions.

IV In the so called *Geiger Müller region*, the positive ions produce an avalanche of ion-pairs. The field strength is so high, that the discharge, once ignited, continues to spread until amplification cannot occur, due to the high density of positive ions around the anode.

V Here the discharge process is not able to stop by itself. only organic gasses like methane or ethanol are able to stop the this discharge process. Its called *discharge region*.

3 Data analysis

3.1 Counter characteristics with ^{238}U

The characteristical $n(U)$ curve of the counter with the ^{238}U sample and the background measurement with the empty aluminium tray are displayed in figure 5

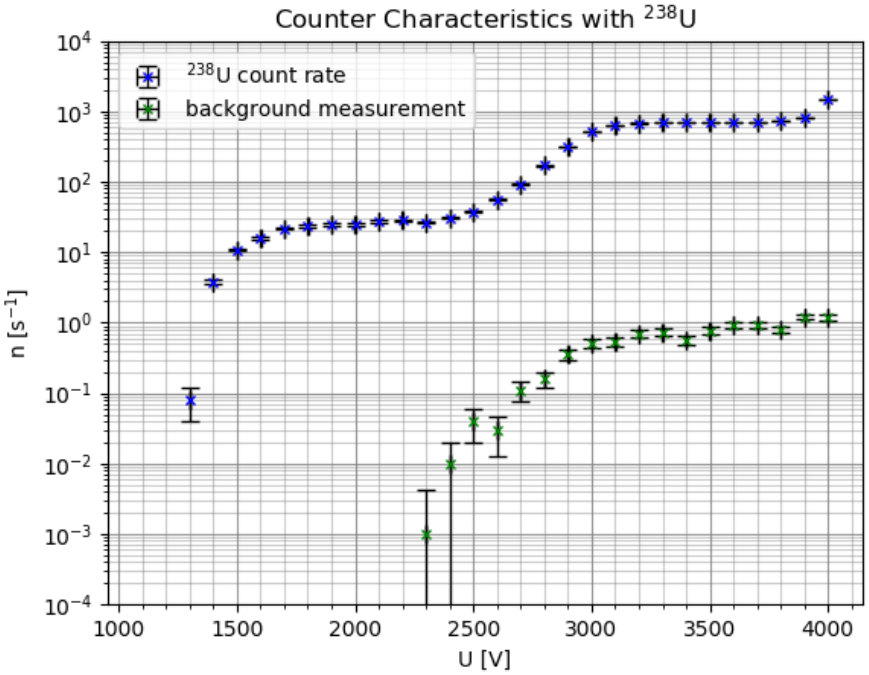

Figure 5: Measured counter characteristics with ^{238}U and background measurement. The count rate n is displayed on a logarithmic scale. The background measurement did not show any counts for $U < 2300$V.

The measurement time Δt for each data point of the ^{238}U count rate was set to $\Delta t = 50$s and for the background measurement $\Delta t_B = 100$s. The respective uncertainties are:

$$s_n = \sqrt{\frac{n}{\Delta t}} \tag{12}$$

$$s_{n_B} = \sqrt{\frac{n_B}{\Delta t_B}} \tag{13}$$

The counter characteristics curve is corrected by the background measurement:

$$n_{corr} = n - n_B \tag{14}$$

$$s_{ncorr} = \sqrt{s_n^2 + s_{n_B}^2} \tag{15}$$

The corrected curve is shown in fig. 6.

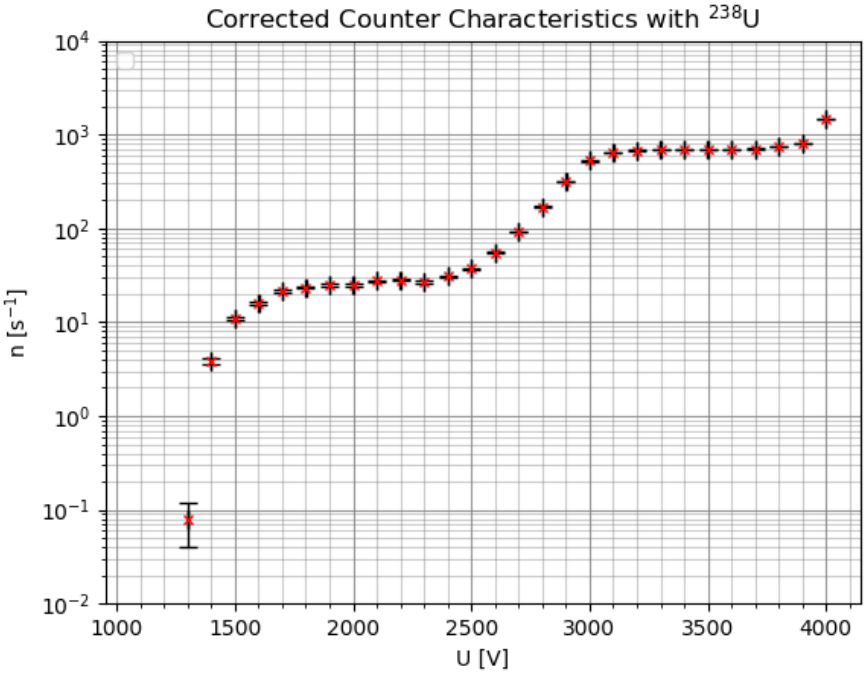

Figure 6: Corrected counter characteristics curve with ^{238}U.

The α plateau is identified at $\sim$ 1900V to $\sim$ 2400V, the β plateau at $\sim$ 3100V to $\sim$ 3800V.

3.2 Determination of the half-Life of ^{147}Sm

To determine the Voltage that has to be applied to operate the detector in the proportional counting region, we measure the counter characteristics curve at the region of the α plateau, and correct it analogously to section 3.1. The data obtained is shown in fig. 7.

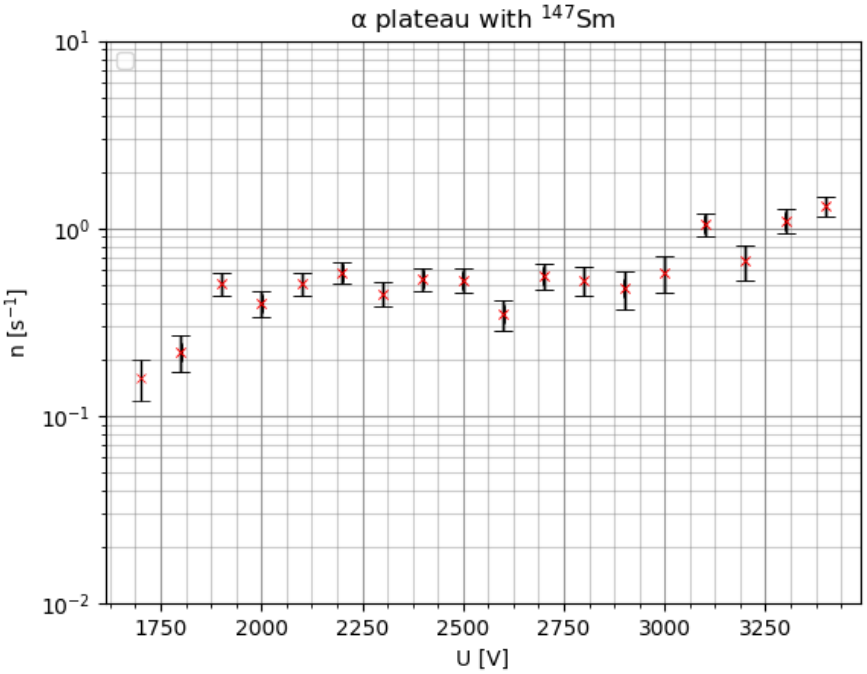

Figure 7: Measurement of the α plateau for ^{147}Sm. The count rate n is displayed on a logarithmic scale.

We identify the α plateau at $\sim$ 1900V to $\sim$ 2400V. Therefore the Voltage applied to the counter for the measurement of the count rate of ^{147}Sm is set to 2300V.

To determine the half-life of ^{147}Sm according to equation 8,

$$T_{1/2} = \frac{\ln(2) \cdot N_\mathrm{A} \cdot h_\mathrm{rel} \cdot F \cdot R_\mathrm{air} \cdot \rho_\mathrm{air}}{2 \cdot n \cdot M_{\mathrm{Sm_2O_3}}} \cdot \sqrt{\frac{m_{\mathrm{A,Sm_2O_3}}}{m_{\mathrm{A,air}}}},$$

we first have to calculate the surface area F. We average our measurements of the inner diameter of the aluminium tray (cf. table 1),

Measurement Nr.	d [cm]
1	2.88 ± 0.05
2	2.88 ± 0.05
3	2.83 ± 0.05
4	2.88 ± 0.05
5	2.88 ± 0.05
6	2.83 ± 0.05
7	2.88 ± 0.05

Table 1: Mesaurements of the inner diameter d of the aluminium tray

which leads to an arithmetic mean of

$$\overline{d} = (2.87 \pm 0.02)\text{cm} \quad , \tag{16}$$

where $s_{\overline{d}} = \frac{s_d}{\sqrt{7}}$.

$\overline{d}$ is used to calculate the surface area F of the ^{147}Sm sample:

$$F = \pi \left(\frac{\overline{d}}{2}\right)^2 \quad . \tag{17}$$

The count rate n is averaged over the measurements taken at a constant measurement time interval $\Delta t = 30$s and counter voltage 2300V, where we weigh the n-values by their respective uncertainty $s_n = \sqrt{\frac{n}{\Delta t}}$ and the count rate of the background measurement n_B likewise. The weighted mean $\overline{n}$ is corrected with the weighted mean $\overline{n_U}$ of the background measurement, which yields

$$\overline{n_{corr}} = \overline{n} - \overline{n_B} = (0.45 \pm 0.16)\text{s}^{-1} \quad , \tag{18}$$

The uncertainty is calculated as follows:

$$s_n = \sqrt{\frac{n}{t}} \tag{19}$$

$$s_{n_B} = \sqrt{\frac{n_B}{t_B}} \tag{20}$$

$$s_{n_{corr}} = \sqrt{s_n^2 + s_{n_B}^2} \quad , \tag{21}$$

where $t = 6000$s and $t_B = 1200$s are the overall measurement times, hence the sum of all time intervals Δt of the respective measurement ($\Delta t_b = 30$s).

With equation 8 and the corrected count rate $\overline{n_{corr}}$, we obtain:

$$\underline{\underline{T_{1/2,\,Sm} = (0.95 \pm 0.03) \cdot 10^{11}\,\text{years}}} \quad , \tag{22}$$

where

$$s_{T_{1/2,\,Sm}} = T_{1/2}\sqrt{\left(\frac{s_F}{F}\right)^2 + \left(\frac{s_{\overline{n_{corr}}}}{n_{corr}}\right)^2} . \tag{23}$$

and the constants used in eq. 8 are

$$N_A = 6.022 \cdot 10^{23}\text{mol}^{-1} \tag{24}$$
$$h_{rel} = 0.1487 \tag{25}$$
$$R_{air} = 1.13\text{cm} \tag{26}$$
$$\rho_{air} = 0.001226\frac{\text{g}}{\text{cm}^3} \tag{27}$$
$$\sqrt{m_{A,\,air}} = 3.833\sqrt{u} \tag{28}$$
$$\sqrt{m_{A,\,air}} = 11.125\sqrt{u}, \tag{29}$$
$$M_{Sm_2O_3} = 2M_{A,\,Sm} + 3M_{A,\,O} = 2 \cdot 150.6\frac{\text{g}}{\text{mol}} + 3 \cdot 15.999\frac{\text{g}}{\text{mol}} = 348.717\frac{\text{g}}{\text{mol}} \tag{30}$$

3.3 Determination of the half-life of ^{40}K

To determine the half-life of ^{40}K, we follow the same procedure as in section 3.2 to calculate $\overline{n_{corr}}$ for each mass. We set the relevant parameters to $\Delta t = 100$s, $t = 800$s, $\Delta t_B = 30$s and $t_B = 1200$s. The region of the β plateau of the counter characteristics curve with the ^{40}K sample is shown in fig. 8.

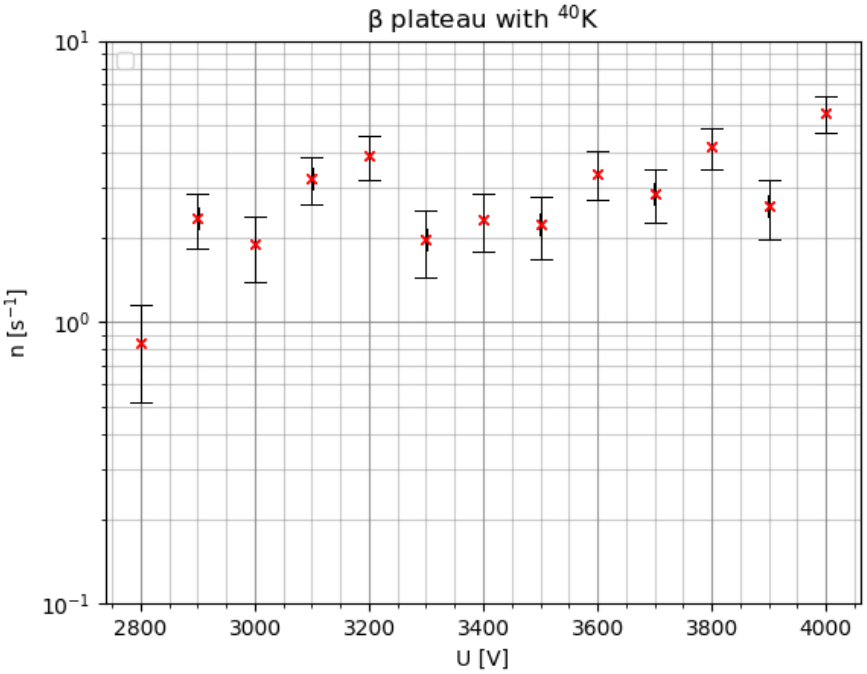

Figure 8: Measurement of the β plateau for ^{40}K.

We identify the β plateau at $\sim$ 2900V to $\sim$ 3700V. The Voltage applied to the counter for the measurement of the count rate of ^{40}K is set to 3500V.

The uncertainty on the mass is estimated to 5 digits: $s_m = \frac{0.0005}{\sqrt{3}}$g to take into account that the scale, which had been gauged to zero before every measurement, often showed values slightly different from zero after the measurement which is possibly caused by dust on the scale. The mass is corrected by the mass of the aluminium tray ($m = m_{uncorr} - m_{tray}$) and the errors of the two weighs quadratically add up to $s_m = \sqrt{\frac{2}{3}} \cdot 0.0005\text{g} = 0.0004\text{g}$. The values obtained are:

$m_{uncorr}[g]$	m [g]	$\overline{n_{corr}}$ [s^{-1}]
1.4681 ± 0.0005	0.1790 ± 0.0004	1.39 ± 0.05
1.5351 ± 0.0005	0.2460 ± 0.0004	1.77 ± 0.05
1.6415 ± 0.0005	0.3524 ± 0.0004	2.31 ± 0.04
1.7456 ± 0.0005	0.4565 ± 0.0004	2.88 ± 0.04
1.8944 ± 0.0005	0.6053 ± 0.0004	3.24 ± 0.04
1.9802 ± 0.0005	0.6911 ± 0.0004	3.80 ± 0.04
2.1826 ± 0.0005	0.8935 ± 0.0004	4.02 ± 0.04
2.3484 ± 0.0005	1.0593 ± 0.0004	4.13 ± 0.04
2.4645 ± 0.0005	1.1754 ± 0.0004	4.45 ± 0.04
2.0956 ± 0.0005	0.8065 ± 0.0004	3.64 ± 0.04

Table 2: Corrected average $\overline{n_{corr}}$ for each mass m

Figure 9 shows a plot of these data points and an exponential fit of the form of eq. 11

$$n(m) = \alpha\,(1 - \exp\{-\beta m\}) \quad .$$

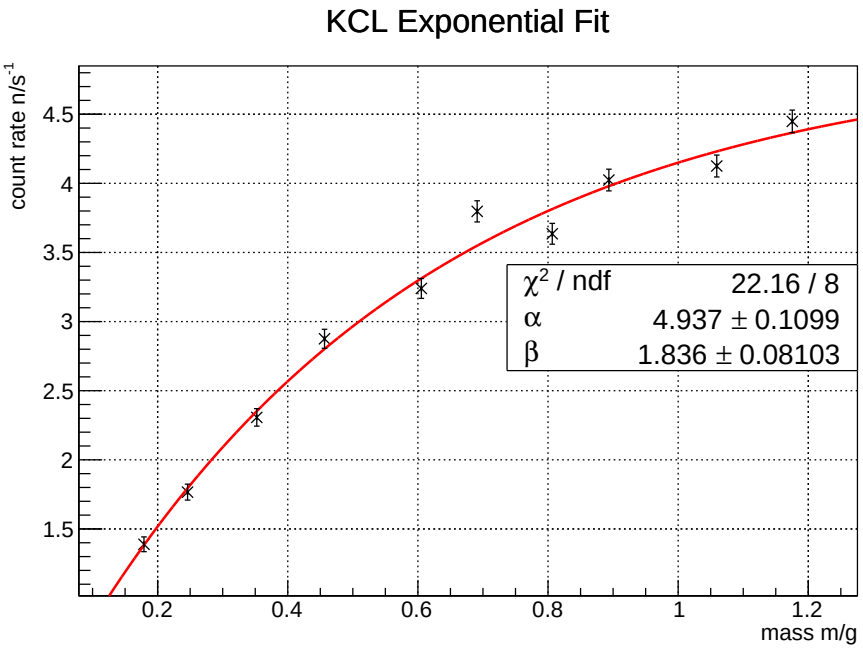

Figure 9: plot of the $\overline{n_{corr}}$ values as a function of m with exponential fit. The mass uncertainties s_m are too small to be seen in the diagram.

The fit yields the following parameters:

$$\alpha = (4.94 \pm 0.11)\mathrm{s}^{-1} \tag{31}$$

$$\beta = (1.84 \pm 0.08)\mathrm{g}^{-1} \tag{32}$$

$$\mathrm{cov} = \begin{pmatrix} 0.01207 & -0.008436 \\ -0.008436 & 0.006566 \end{pmatrix} \tag{33}$$

The fit parameters α and β kan be inserted into the formula for the half-life of Potassium (Equation 10):

$$\underline{\underline{T_{1/2,\,K}}} = \frac{\ln(2)_A \cdot h_{rel}}{1.12 \cdot A_S \cdot M_{KCL}} = \frac{f_B \cdot \log(2) \cdot N_A \cdot h_{rel}}{1.12 \cdot 2 \cdot \alpha \cdot \beta \cdot M_{KCl}} \tag{34}$$

$$= \underline{\underline{(1.33 \pm 0.03) \cdot 10^9 \,\text{years}}} \quad , \tag{35}$$

where

$$s_{T_{1/2,\,K}} = \sqrt{\left(\frac{\partial T_{1/2,\,K}}{\partial \alpha}, \frac{\partial T_{1/2,\,K}}{\partial \beta}\right) \cdot \text{cov} \cdot \left(\frac{\partial T_{1/2,\,K}}{\partial \alpha}, \frac{\partial T_{1/2,\,K}}{\partial \beta}\right)^T} \tag{36}$$

and

$$\frac{\partial T_{1/2,\,K}}{\partial \alpha} = -\frac{T_{1/2,\,K}}{\alpha} \tag{37}$$

$$\frac{\partial T_{1/2,\,K}}{\partial \beta} = -\frac{T_{1/2,\,K}}{\beta} \quad . \tag{38}$$

and the constants used in the formula are

$$h_{rel} = 0.000188, \quad f_B = 1.29, \quad M_{KCl} = 74.55, N_A = 6.022 \cdot 10^{21}\text{mol}^{-1} \tag{39}$$

4 Summary and discussion of results

In this experiment, we first obtained the characteristic curve of the gaseous ionisation counter using a ^{238}U sample which led to the expected result. We then operated the counter in its proportional counting region to measure the count rate of the α decay of the ^{147}Sm isotope in Sm_2O_3 and the count rate of the β decay of the ^{40}K isotope in KCl. We then exploited the constant range of α radiation and the dependence of the activity A of α radiation sources of the surface area of the Sm_2O_3 sample to determine the half-life $T_{1/2}$ of ^{147}Sm. To determine the half-life of ^{40}K we exploited the mass dependence of the activity A.

We obtained the following values:

$$^{147}\text{Sm}: \quad T_{1/2,\,^{147}\text{Sm}} = (0.95 \pm 0.03) \cdot 10^{11}\,\text{years} \tag{40}$$

$$^{40}\text{K}: \quad T_{1/2,\,^{40}\text{K}} = (1.33 \pm 0.03) \cdot 10^{9}\,\text{years} \tag{41}$$

The value for ^{147}Sm coincides with the reference value $T_{1/2,\,^{147}\text{Sm}} = 1.06 \cdot 10^{11}$ years[1] within 4σ. The value for ^{40}K coincides with the reference value $T_{1/2,\,^{40}\text{K}} = 1.28 \cdot 10^{9}$ years [1] within 2σ.

We suspect the high discrepancy of the result for ^{147}Sm to be caused by contamination of the Sm_2O_3 with foreign substances since the same bottle is used by every group and the material is put back into the bottle every time. Another reason for the too small result for ^{147}Sm could also be the measurement of the surface area, which does not consider the uneven surface of the crystalline Sm_2O_3. Furthermore, a longer measurement time could help to average out even more statistical events during the measurement.

5 Appendix

5.1 Derivation of the half life formulas

The pictures are taken from [1] and also derivation is inspired by [1].

5.1.1 $T_{1/2}$ of ^{147}Sm

Because α-emitters have a small range, the Equation 7 has to be corrected by a specific factor, which we try to derive here. Due to the small range, not all α particles reach the outside of the sample. The geometrical correlation between the range and thickness of the sample is as shown in Figure 10 the following and limits the the solid angle dΩ:

$$\theta_{max} = \arccos\left(\frac{x}{R}\right) \tag{42}$$

$$d\Omega(x) = \int_0^{2\pi} \varphi \int_0^{\theta_{max}} \sin(\theta) d\theta = 2\pi\left(1 - \frac{x}{R}\right) \tag{43}$$

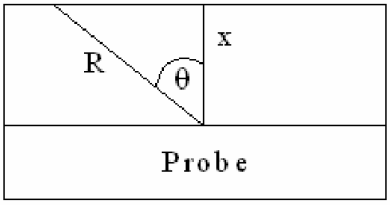

Figure 10: Relation between solid angle Ω and the range R inside the sample

The rate of counts can then be obtained by the following integral as:

$$n = \frac{A}{d} \cdot \int_0^R \frac{\Omega}{4\pi} dx = A_v \frac{F}{4} R_{Sm_2O_3} \tag{44}$$

But as sadly $R_{Sm_2O_3}$ is not known, we have to use a ralation by Bragg and Kleemann which states:a

$$R \cdot \rho = \sqrt{m_\alpha} \tag{45}$$

hereby is m_α the effective atomic weight and ρ the density. If we want to calculate the half life of $^{147}_{62}$Sm only with known quantities, we need to introduce more relevant relations. such as the trivial ones

$$\frac{m}{d} = \frac{V\rho}{d} = F \cdot \rho \tag{46}$$

$$N = 2 \cdot N_{Sm_2O_3 \cdot h_{rel}}. \tag{47}$$

where h_{rel} gives the relative amount of ^{147}Sm in Sm_2O_3 and the number of samarium(III)-oxid nuclei is given through:

$$N_{Sm_2O_3} = \frac{m \cdot N_A}{M_{Sm_2O_3}} \tag{48}$$

Hereby stands $N_A$for the Avogardo-constant and $\mathrm{M}_{Sm_2O_3}$ the Molar mass. Therefore we obtain the following:

$$T_{1/2} = \frac{\ln(2) \cdot N_{Sm_2O_3} \cdot h_{rel} \cdot R_{Sm_2O_3}}{2 \cdot n \cdot d} \tag{49}$$

$$= \frac{\ln(2) \cdot N_A \cdot h_{rel} \cdot R_{Sm_2O_3} \cdot \rho_{Sm_2O_3} \cdot F}{2 \cdot n \cdot M_{Sm_2O_3}} \tag{50}$$

$$= \frac{\ln(2) \cdot N_\mathrm{A} \cdot h_\mathrm{rel} \cdot F \cdot R_\mathrm{air} \cdot \rho_\mathrm{air}}{2 \cdot n \cdot M_{\mathrm{Sm_2O_3}}} \cdot \sqrt{\frac{m_{\mathrm{A,Sm_2O_3}}}{m_{\mathrm{A,air}}}} \tag{51}$$

5.1.2 $T_{1/2}$ of ^{40}K

For a infenitessimal small element of mass, which sits in a depth x the rate of cou nts dn is equal to:

$$\begin{aligned} dn &= A_s \cdot e^{-\mu \cdot x} dm \\ &= A_s \cdot \rho e^{-\mu \cdot x} dV \\ &= A_s \cdot \rho F \cdot e^{-\mu \cdot x} dx \end{aligned} \tag{52}$$

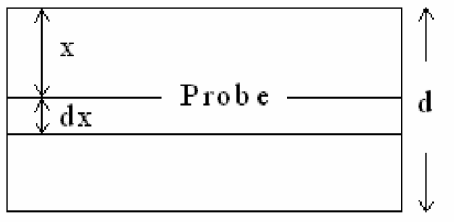

Figure 11: Relation between the volume elements dx, the thickness d and the distance$x$ to the surface of the sample.

Integrating over the thickness results in:

$$n = \frac{A_s \cdot \rho \cdot F}{\mu} \left((1 - e^{--\mu \cdot d} \right) \tag{53}$$

Now one can substitute d with $d = \frac{m}{\rho \cdot f}$ then we end up with the following:

$$n = \frac{f_B \cdot j A_S \cdot \rho \cdot F}{2\mu} \left(1 - e^{-\frac{\mu \cdot m}{\rho \cdot F}} \right) \tag{54}$$

The factor $\frac{f_b}{2}$ (f_B=1.19) is a constant for the reflecting properties of the aluminium tray. the unknown quantities A_S and μ can be calculated with the fit function Figure 9.

$$A_S = \frac{2 \cdot \mu \cdot \alpha}{f_B \cdot \rho \cdot F} = \frac{2\alpha \cdot \beta}{f_B} \tag{55}$$

References

[1] Tobijas Kotyk *Versuche zur Radioaktivität im Physikalischen Fortgeschrittenen Praktikum an der Albert-Ludwigs-Universität Freiburg 2005*

[2] Picture taken from:
`https://en.wikipedia.org/wiki/List_of_Feynman_diagrams#/media/File:Beta_Negative_Decay.svg` *19.09.2018 14:00*

[3] Picture taken from:
`https://classconnection.s3.amazonaws.com/815/flashcards/2276815/jpg/elec-capture1356714896919-thumb400.jpg`

[4] Jacob Snäll *Tests and simulations of GEM foils for use in an active target gaseous detector; Master Thesis Lund University Feb 2016*